Chin. Phys. B Vol. 29, No. 2 (2020) 020304

Quantifying non-classical correlations under thermal effects in a double cavity optomechanical system

Mohamed Amazioug[1,2,†], Larbi Jebli[3], Mostafa Nassik[3], and Nabil Habiballah[3,4,5]

[1] Department of Physics, Ecole Normale Supérieure (ENS), Mohammed V University in Rabat, Morocco
[2] LPHE-MS, Department of Physics, Faculty of Sciences, Mohammed V University, Rabat, Morocco
[3] EPTHE, Department of Physics, Faculty of Sciences, Ibn Zohr University, Agadir, Morocco
[4] Faculty of Applied Sciences, Ibn Zohr University, Ait-Melloul, Morocco
[5] Abdus Salam International Center for Theoretical Physics, Strada Costiera, 11, 34151, Trieste, Italy

(Received 5 October 2019; revised manuscript received 15 December 2019; published online 27 December 2019)

We investigate the generation of quantum correlations between mechanical modes and optical modes in an optomechanical system, using the rotating wave approximation. The system is composed of two Fabry–Pérot cavities separated in space; each of the two cavities has a movable end-mirror. Our aim is the evaluation of entanglement between mechanical modes and optical modes, generated by correlations transfer from the squeezed light to the system, using Gaussian intrinsic entanglement as a witness of entanglement in continuous variables Gaussian states, and the quantification of the degree of mixedness of the Gaussian states using the purity. Then, we quantify nonclassical correlations between mechanical modes and optical modes even beyond entanglement by considering Gaussian geometric discord via the Hellinger distance. Indeed, entanglement, mixdness, and quantum discord are analyzed as a function of the parameters characterizing the system (thermal bath temperature, squeezing parameter, and optomechanical cooperativity). We find that, under thermal effect, when entanglement vanishes, purity and quantum discord remain nonzero. Remarkably, the Gaussian Hellinger discord is more robust than entanglement. The effects of the other parameters are discussed in detail.

Keywords: cavity optomechanics, quantum correlations, Gaussian intrinsic entanglement, purity, Gaussian Hellinger discord, Gaussian geometric discord

PACS: 03.65.–w, 42.50.–p, 42.50.Ex **DOI:** 10.1088/1674-1056/ab65b6

1. Introduction

Entanglement[1–3] is a fundamental feature of quantum mechanics, which plays a crucial role in different applications of quantum information processing, such as quantum teleportation,[4] superdense coding,[5] telecloning,[6] and quantum cryptography.[7] In optomechanical systems, entanglement is due to the interaction between the movable mirror and the radiation field via the radiation pressure.[8–10] Recently, several studies have been conducted to investigate entanglement and quantum correlations in optomechanical systems.[11–17] But the entanglement is very fragile under the thermal effect when the quantum system interacts with its environment; it is a decoherence phenomenon.[18] Moreover, in optomechanical systems, it has been found that the entanglement disappears rapidly under the effect of certain parameters; it is the entanglement sudden death (ESD) phenomenon.[19] This phenomenon occurs when the entangled multipartite quantum system is placed in Markovian environments.[20–24]

In this paper, we use a system consisting of two spatially separated Fabry–Pérot cavities, each cavity having a movable end-mirror (as shown in Fig. 1). Our objective is to study the quantum correlations between mirror 1–mirror 2 and optical 1–optical 2 modes in this system, by making use of the rotating wave approximation. Thus, after derivations of the steady state of the mechanical and optical modes of two-mode continuous variables Gaussian states, we will analyze Gaussian intrinsic entanglement and Gaussian geometric discord in terms of Hellinger distance to quantify quantum correlations, while as the purity to quantify the mixedness between mechanical and optical modes.

The rest of the present article is organized as follows. In Section 2, we describe the model and the system under investigations, we also give the expression of the Hamiltonian and the quantum nonlinear Langevin equations (QLEs) for the mechanical and optical modes. In Section 3, we linearize the QLEs and derive the quantum equations that govern the dynamics of the system. In Section 4, in Gaussian state of continuous variables we calculate the covariance matrix of the system in the steady state. Then, we study the Gaussian intrinsic entanglement[25] to measure the quantum correlations between mechanical and optical modes, and the purity to measure the mixedness[25,26] (Section 5). Finally, we use also the Gaussian geometric discord in terms of the Hellinger distance to characterize the quantum correlations beyond the entanglement between mechanical and optical modes[28] (Section 6). Conclusions close the paper.

†Corresponding author. E-mail: amazioug@gmail.com

 http://iopscience.iop.org/cpbhttp://cpb.iphy.ac.cn

2. Model

We consider two Fabry–Pérot cavities composed of a fixed mirror (spatially transmitting) and a movable mirror M_p ($p = 1,2$) (perfectly reflecting). The mass and the frequency of the p^{th} movable mirror are respectively m_p and ω_{M_p}. As illustrated in Fig. 1, the cavities are coupled to a common two-mode squeezed light from the output of the parametric down conversion, and are pumped by coherent laser field which is coupled to the movable mirror M_1 (M_2) via radiation pressure with the coupling rate $g_p = (\omega_{a_p}/L_p)\sqrt{\hbar/m_p\omega_{M\,p}}$,[10] where L_p is the p^{th} cavity length.

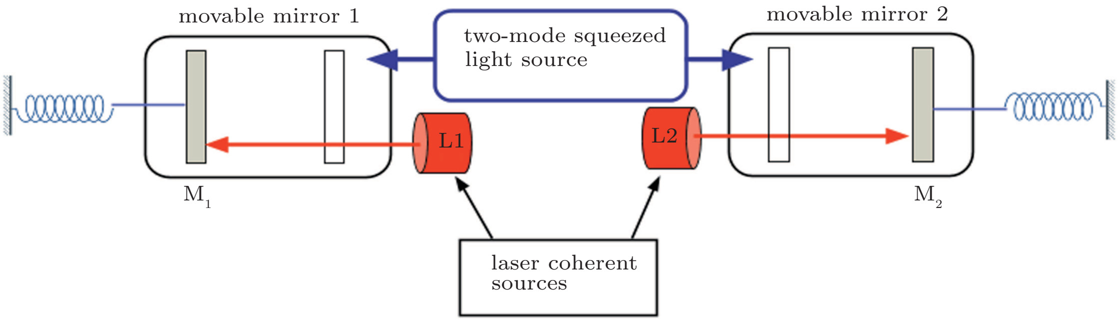

Fig. 1. The schematic diagram of two identical Fabry–Pérot cavities coupled to a two-mode squeezed light from spontaneous parametric down-conversion and driven by coherent laser sources with amplitude ε_p and the squeezed vacuum.

The system Hamiltonian in frame rotating with ω_{Lp} is given by[12]

$$\mathcal{H} = \sum_{p=1}^{2}\left[\hbar\omega_{M_p}d_p^\dagger d_p + \hbar(\omega_{a_p}-\omega_{L_p})a_p^\dagger a_p + \hbar g_p a_p^\dagger a_p(d_p^\dagger + d_p) + \hbar(a_p^\dagger\varepsilon_p\,\mathrm{e}^{\mathrm{i}\phi_p} + a_p\varepsilon_p\,\mathrm{e}^{-\mathrm{i}\phi_p})\right], \tag{1}$$

where ω_{a_p} is the p^{th} cavity frequency, ϕ_p and $\varepsilon_p = \sqrt{2\kappa_p\mathcal{P}_p/\hbar\omega_{L\,p}}$ ($p = 1,2$) are respectively the phase and the input coherent field. κ_p is the cavity damping rate, $\mathcal{P}_p$ is the driving pump power, $\omega_{L\,p}$ is the frequency of the p^{th} input field. The mechanical modes are considered as quantum harmonic oscillators, with annihilation and creation operators d_p and $d_p^\dagger$ satisfying the commutation relations $[d_p, d_p^\dagger] = 1$ ($p = 1,2$). a_p and $a_p^\dagger$ are the annihilation and creation operators of the p^{th} cavity mode, with $[a_p, a_p^\dagger] = 1$ ($p = 1,2$).

Considering the Hamiltonian Eq. (1), the nonlinear quantum Langevin equations, describing the dynamics of the movable mirrors and optical modes are written by[29–31]

$$\dot{d}_p = -\left(\mathrm{i}\omega_{M_p} + \frac{\gamma_p}{2}\right)d_p - \mathrm{i}g_p a_p^\dagger a_p + \sqrt{\gamma_p}d_p^{\text{in}}, \tag{2}$$

$$\dot{a}_p = -\left(\frac{\kappa_p}{2} - \mathrm{i}\Delta_p\right)a_p - \mathrm{i}g_p a_p(d_p^\dagger + d_p) - \mathrm{i}\varepsilon_p\,\mathrm{e}^{\mathrm{i}\phi_p} + \sqrt{\kappa_p}a_p^{\text{in}} \tag{3}$$

with γ_p and $\Delta_p = \omega_{L_p} - \omega_{a_p}$ are respectively the mechanical damping rate and laser detuning ($p = 1,2$), d_p^{in} is the p^{th} noise operator describing the coupling between mechanical mode and its own environment and a_p^{in} is the squeezed vacuum operator.

For a large value of the mechanical quality factor, it can be assumed that the mechanical baths are Markovian. The nonzero correlation function[32,33] is given by

$$\langle d_p^{\text{in}}(t)d_p^{\text{in}\dagger}(t')\rangle = (n_{\text{th}_p}+1)\delta(t-t'), \tag{4}$$

$$\langle d_p^{\text{in}\dagger}(t)d_p^{\text{in}}(t')\rangle = n_{\text{th}_p}\delta(t-t'), \tag{5}$$

where the thermal baths photons numbers in the p^{th} cavity is

$$n_{\text{th}_p} = \left[\exp\left(\frac{\hbar\omega_{M_p}}{k_{\text{B}}T_p}\right) - 1\right]^{-1}$$

with k_{B} being the Boltzmann constant.

The squeezed vacuum operators a_p^{in} and $a_p^{\text{in}\dagger}$ have nonzero correlation properties[34]

$$\langle a_p^{\text{in}}(t)a_p^{\text{in}\dagger}(t')\rangle = (\mathcal{N}+1)\delta(t-t'), \tag{6}$$

$$\langle a_p^{\text{in}\dagger}(t)a_p^{\text{in}}(t')\rangle = \mathcal{N}\delta(t-t'), \tag{7}$$

$$\langle a_q^{\text{in}}(t)a_p^{\text{in}}(t')\rangle = \mathcal{M}\,\mathrm{e}^{-\mathrm{i}\omega_M(t+t')}\delta(t-t'), \quad q \neq p, \tag{8}$$

$$\langle a_q^{\text{in}\dagger}(t)a_p^{\text{in}\dagger}(t')\rangle = \mathcal{M}\,\mathrm{e}^{\mathrm{i}\omega_M(t+t')}\delta(t-t'), \quad q \neq p, \tag{9}$$

where $\mathcal{N} = \sinh^2 r$ and $\mathcal{M} = \sqrt{\mathcal{N}(\mathcal{N}+1)}$ with r being the squeezing parameter characterizing the squeezed light (we consider $\omega_M = \omega_{M_1} = \omega_{M_2}$).

3. Linearization of quantum Langevin equations

The nonlinear quantum Langevin equations are in general non-solvable analytically. In this way, we use the scheme of linearization given in Ref. [35]

$$d_p = \bar{d}_p + \delta d_p, \qquad a_p = \bar{a}_p + \delta a_p, \tag{10}$$

where δd_p and δa_p are the operators of fluctuations. $\bar{d}_p$ and $\bar{a}_p$ are respectively the mean values of the operators d_p and a_p. Considering Eqs. (2) and (3) in its steady state, one can obtain

$$\bar{a}_p = \frac{-\mathrm{i}\varepsilon_p\,\mathrm{e}^{\mathrm{i}\phi_p}}{\kappa_p/2 - \mathrm{i}\Delta_p'}, \tag{11}$$

$$\bar{d}_p = \frac{-\mathrm{i} g_p \mid \bar{a}_p \mid^2}{\gamma_p/2 + \mathrm{i}\omega_{M_p}}, \tag{12}$$

where $\Delta'_p = \Delta_p - g_p(\bar{d}_p + \bar{d}^*_p)$, is considered as the effective cavity detuning which depends on the displacement of the mirrors due to the radiation pressure force. Replacing $d_p = \bar{d}_p + \delta d_p$ and $a_p = \bar{a}_p + \delta a_p$ in Eqs. (2) and (3), thus

$$\begin{aligned} \delta\dot{d}_p &= -\left(\mathrm{i}\omega_{M_p} + \frac{\gamma_p}{2}\right)\delta d_p \\ &\quad + \mathcal{G}_p(\delta a_p - \delta a^\dagger_p) + \sqrt{\gamma_p} d^{\mathrm{in}}_p, \end{aligned} \tag{13}$$

$$\begin{aligned} \delta\dot{a}_p &= -\left(\frac{\kappa_p}{2} - \mathrm{i}\Delta'_p\right)\delta a_p \\ &\quad - \mathcal{G}_p(\delta d^\dagger_p + \delta d_p) + \sqrt{\kappa_p} a^{\mathrm{in}}_p, \end{aligned} \tag{14}$$

where $\mathcal{G}_p = g_p \mid \bar{a}_p \mid$ is the many-photon optomechanical coupling inside the p^{th} cavity, ϕ_p is the arbitrary phase of p^{th} input laser $\phi_p = -\arctan(2\Delta'_p/\kappa_p)$ and $\bar{a}_p = -\mathrm{i} \mid \bar{a}_p \mid$. Using the notations $\delta a_p(t) = \delta\tilde{a}_p(t)\,\mathrm{e}^{\mathrm{i}\Delta'_p t}$, $\delta d_p(t) = \delta\tilde{d}_p(t)\,\mathrm{e}^{-\mathrm{i}\omega_{M_p} t}$, $\tilde{a}^{\mathrm{in}}_p = \mathrm{e}^{-\mathrm{i}\Delta'_p t} a^{\mathrm{in}}_p$, and $\tilde{d}^{\mathrm{in}}_p = \mathrm{e}^{\mathrm{i}\omega_{M_p} t} d^{\mathrm{in}}_p$, equations (13) and (14) became

$$\begin{aligned} \delta\dot{\tilde{d}}_p &= -\frac{\gamma_p}{2}\delta\tilde{d}_p + \mathcal{G}_p\left(\delta\tilde{a}_p\,\mathrm{e}^{\mathrm{i}(\Delta'_p + \omega_{M_p})t} - \delta\tilde{a}^+_p\,\mathrm{e}^{-\mathrm{i}(\Delta'_p - \omega_{M_p})t}\right) \\ &\quad + \sqrt{\gamma_p}\tilde{b}^{\mathrm{in}}_p, \end{aligned} \tag{15}$$

$$\begin{aligned} \delta\dot{\tilde{a}}_p &= -\frac{\kappa_p}{2}\delta\tilde{a}_p - \mathcal{G}_p\left(\delta\tilde{d}^+_p\,\mathrm{e}^{-\mathrm{i}(\Delta'_p - \omega_{M_p})t} + \delta\tilde{d}_p\,\mathrm{e}^{-\mathrm{i}(\Delta'_p + \omega_{M_p})t}\right) \\ &\quad + \sqrt{\kappa_p}\tilde{a}^{\mathrm{in}}_p. \end{aligned} \tag{16}$$

Using the rotating wave approximation (RWA)[10,36] (*i.e.*, $\omega_{M_p} \gg \kappa_p$ with $p = 1,2$), the effective cavity detuning is reduced to $\Delta'_p \approx \Delta_p$, and one can neglect the terms rotating at $\pm 2\omega_{M_p}$. When the cavity is driven at the red sideband ($\Delta'_p = -\omega_{M_p}$ with $p = 1,2$), equations (15) and (16) become

$$\begin{pmatrix} \delta\dot{\tilde{d}}_p \\ \delta\dot{\tilde{a}}_p \end{pmatrix} = \begin{pmatrix} -\gamma_p/2 & \mathcal{G}_p \\ -\kappa_p/2 & -\mathcal{G}_p \end{pmatrix} \begin{pmatrix} \delta\tilde{d}_p \\ \delta\tilde{a}_p \end{pmatrix} + \begin{pmatrix} \sqrt{\gamma_p}\tilde{d}^{\mathrm{in}}_p \\ \sqrt{\kappa_p}\tilde{a}^{\mathrm{in}}_p \end{pmatrix}. \tag{17}$$

4. Steady state covariance matrix

The linear quantum Langevin equations allow us to deduce the covariance matrix (CM) that describes the evolution of the steady state of the system, then to characterize purity, entanglement, and beyond entanglement between various modes by making use of different criteria and quantifiers of correlations.

For the sake of simplicity, we consider that the two coherent sources have identical strength, and the thermal baths of two mechanical mirrors are at the same temperature $T_1 = T_2 = T$ ($n_{\mathrm{th}_1} = n_{\mathrm{th}_2} = n_{\mathrm{th}}$). Furthermore, $m_1 = m_2 = m$, $\omega_{r_1} = \omega_{r_2} = \omega_r$, $\omega_{\mathrm{M}_1} = \omega_{\mathrm{M}_2} = \omega_{\mathrm{M}}$, $\kappa_1 = \kappa_2 = \kappa$, and $\gamma_1 = \gamma_2 = \gamma$.

To derive the explicit formula of the CM for continuous variables, we consider the EPR-type quadrature operators for the two subsystems

$$\delta\tilde{Q}_{d_p} = \frac{\delta\tilde{d}^\dagger_p + \delta\tilde{d}_p}{\sqrt{2}}, \quad \delta\tilde{P}_{d_p} = \frac{\delta\tilde{d}_p - \delta\tilde{d}^\dagger_p}{\mathrm{i}\sqrt{2}}, \quad p = 1,2, \tag{18}$$

$$\delta\tilde{Q}_{a_p} = \frac{\delta\tilde{a}^\dagger_p + \delta\tilde{a}_p}{\sqrt{2}}, \quad \delta\tilde{P}_{a_p} = \frac{\delta\tilde{a}_p - \delta\tilde{a}^\dagger_p}{\mathrm{i}\sqrt{2}}, \quad p = 1,2. \tag{19}$$

Equation (17) becomes in terms of quadrature operators[14]

$$\delta\dot{\tilde{Q}}_{d_p} = -\frac{\gamma}{2}\delta\tilde{Q}_{d_p} + \mathcal{G}\delta\tilde{Q}_{a_p} + \sqrt{\gamma}\tilde{Q}^{\mathrm{in}}_{d_d}, \quad p = 1,2, \tag{20}$$

$$\delta\dot{\tilde{P}}_{d_p} = -\frac{\gamma}{2}\delta\tilde{P}_{d_p} + \mathcal{G}\delta\tilde{P}_{a_p} + \sqrt{\gamma}\tilde{P}^{\mathrm{in}}_{d_p}, \quad p = 1,2, \tag{21}$$

$$\delta\dot{\tilde{Q}}_{a_p} = -\frac{\kappa}{2}\delta\tilde{Q}_{a_p} - \mathcal{G}\delta\tilde{Q}_{d_p} + \sqrt{\kappa}\tilde{Q}^{\mathrm{in}}_{a_p}, \quad p = 1,2, \tag{22}$$

$$\delta\dot{\tilde{P}}_{a_p} = -\frac{\kappa}{2}\delta\tilde{P}_{a_p} - \mathcal{G}\delta\tilde{P}_{d_p} + \sqrt{\kappa}\tilde{P}^{\mathrm{in}}_{a_p}, \quad p = 1,2 \tag{23}$$

with

$$\tilde{Q}^{\mathrm{in}}_{d_p} = \frac{\tilde{d}^{\mathrm{in}\,\dagger}_p + \tilde{d}^{\mathrm{in}}_p}{\sqrt{2}}, \quad \tilde{P}^{\mathrm{in}}_{d_p} = \frac{\tilde{d}^{\mathrm{in}}_p - \tilde{d}^{\mathrm{in}\,\dagger}_p}{\mathrm{i}\sqrt{2}}, \quad p = 1,2, \tag{24}$$

$$\tilde{Q}^{\mathrm{in}}_{a_p} = \frac{\tilde{a}^{\mathrm{in}\,\dagger}_p + \tilde{a}^{\mathrm{in}}_p}{\sqrt{2}}, \quad \tilde{P}^{\mathrm{in}}_{a_p} = \frac{\tilde{a}^{\mathrm{in}}_p - \tilde{a}^{\mathrm{in}\,\dagger}_p}{\mathrm{i}\sqrt{2}}, \quad p = 1,2. \tag{25}$$

Equations (20)–(23) are given in a compact matrix[37]

$$\dot{u}(t) = \mathcal{A}u(t) + \lambda(t) \tag{26}$$

with the following form of

$$\begin{aligned} u^{\mathrm{T}}(t) &= \left(\delta\tilde{Q}_{d_1}, \delta\tilde{P}_{d_1}, \delta\tilde{Q}_{d_2}, \delta\tilde{P}_{d_2}, \delta\tilde{Q}_{a_1}, \delta\tilde{P}_{a_1}, \delta\tilde{Q}_{a_2}, \delta\tilde{P}_{a_2}\right), \\ \lambda^{\mathrm{T}}(t) &= \left(\sqrt{\gamma}\tilde{Q}^{\mathrm{in}}_{d_1}, \sqrt{\gamma}\tilde{P}^{\mathrm{in}}_{d_1}, \sqrt{\gamma}\tilde{Q}^{\mathrm{in}}_{d_2}, \sqrt{\gamma}\tilde{P}^{\mathrm{in}}_{d_2}, \sqrt{\kappa}\tilde{Q}^{\mathrm{in}}_{a_1}, \sqrt{\kappa}\tilde{P}^{\mathrm{in}}_{a_1}, \sqrt{\kappa}\tilde{Q}^{\mathrm{in}}_{a_2}, \sqrt{\kappa}\tilde{P}^{\mathrm{in}}_{a_2}\right), \end{aligned}$$

where

$$\mathcal{A} = \begin{pmatrix} -\gamma/2 & 0 & 0 & 0 & \mathcal{G} & 0 & 0 & 0 \\ 0 & -\gamma/2 & 0 & 0 & 0 & \mathcal{G} & 0 & 0 \\ 0 & 0 & -\gamma/2 & 0 & 0 & 0 & \mathcal{G} & 0 \\ 0 & 0 & 0 & -\gamma/2 & 0 & 0 & 0 & \mathcal{G} \\ -\mathcal{G} & 0 & 0 & 0 & -\kappa/2 & 0 & 0 & 0 \\ 0 & -\mathcal{G} & 0 & 0 & 0 & -\kappa/2 & 0 & 0 \\ 0 & 0 & -\mathcal{G} & 0 & 0 & 0 & -\kappa/2 & 0 \\ 0 & 0 & 0 & -\mathcal{G} & 0 & 0 & 0 & -\kappa/2 \end{pmatrix}. \tag{27}$$

Since all eigenvalues of the drift matrix $\mathcal{A}$ are negative (for $\mathcal{G} > \kappa, \gamma$, *i.e.*, $2\mathcal{G} > \kappa + \gamma$), the system under study is stable.[38] The steady state of the system can be described by the covariance matrix whose form is $\mathbb{V}_{ij} = (1/2)(\langle u_i(t)u_j(t') + u_j(t')u_i(t)\rangle)$. Then, the covariance matrix in steady state can be derived by considering Lyapunov equation, given by[39,40]

$$\mathcal{A}\mathbb{V} + \mathbb{V}\mathcal{A}^{\mathrm{T}} = -\mathfrak{D} \tag{28}$$

with $\mathfrak{D}$ being the matrix of stationary noise correlations, whose elements are $\mathfrak{D}_{mn}\delta(t-t') = (1/2)(\langle\lambda_m(t)\lambda_n(t') + \lambda_n(t')\lambda_m(t)\rangle)$, the explicit expression of $\mathfrak{D}$ is

$$\mathfrak{D} = \begin{pmatrix} \gamma' & 0 & 0 & 0 & 0 & 0 & 0 & 0 \\ 0 & \gamma' & 0 & 0 & 0 & 0 & 0 & 0 \\ 0 & 0 & \gamma' & 0 & 0 & 0 & 0 & 0 \\ 0 & 0 & 0 & \gamma' & 0 & 0 & 0 & 0 \\ 0 & 0 & 0 & 0 & \kappa' & 0 & \mathcal{M}\kappa & 0 \\ 0 & 0 & 0 & 0 & 0 & \kappa' & 0 & -\mathcal{M}\kappa \\ 0 & 0 & 0 & 0 & \mathcal{M}\kappa & 0 & \kappa' & 0 \\ 0 & 0 & 0 & 0 & 0 & -\mathcal{M}\kappa & 0 & \kappa' \end{pmatrix}, \tag{29}$$

where $\gamma' = \gamma(n_{\text{th}} + 1/2)$ and $\kappa' = \kappa(\mathcal{N} + 1/2)$.

The covariance matrix in steady state is given by

$$\mathbb{V} = \begin{pmatrix} \mathbb{V}_1 & 0 & \mathbb{V}_{13} & 0 & \mathbb{V}_{15} & 0 & \mathbb{V}_{17} & 0 \\ 0 & \mathbb{V}_1 & 0 & -\mathbb{V}_{13} & 0 & \mathbb{V}_{15} & 0 & -\mathbb{V}_{17} \\ \mathbb{V}_{13} & 0 & \mathbb{V}_1 & 0 & \mathbb{V}_{17} & 0 & \mathbb{V}_{15} & 0 \\ 0 & -\mathbb{V}_{13} & 0 & \mathbb{V}_1 & 0 & -\mathbb{V}_{17} & 0 & \mathbb{V}_{15} \\ \mathbb{V}_{15} & 0 & \mathbb{V}_{17} & 0 & \mathbb{V}_2 & 0 & \mathbb{V}_{57} & 0 \\ 0 & \mathbb{V}_{15} & 0 & -\mathbb{V}_{17} & 0 & \mathbb{V}_2 & 0 & -\mathbb{V}_{57} \\ \mathbb{V}_{17} & 0 & \mathbb{V}_{15} & 0 & \mathbb{V}_{57} & 0 & \mathbb{V}_2 & 0 \\ 0 & -\mathbb{V}_{17} & 0 & \mathbb{V}_{15} & 0 & -\mathbb{V}_{57} & 0 & \mathbb{V}_2 \end{pmatrix}. \tag{30}$$

For the two-mode symmetric squeezed thermal states, the covariance matrix for each subsystem (mirror 1–mirror 2 and optic 1–optic 2), can be derived considering the global covariance matrix Eq. (30)

$$\mathbb{V}_{(m_1m_2)} = \begin{pmatrix} \mathbb{V}_1 & 0 & \mathbb{V}_{13} & 0 \\ 0 & \mathbb{V}_1 & 0 & -\mathbb{V}_{13} \\ \mathbb{V}_{13} & 0 & \mathbb{V}_1 & 0 \\ 0 & -\mathbb{V}_{13} & 0 & \mathbb{V}_1 \end{pmatrix},$$
$$\mathbb{V}_{(o_1o_2)} = \begin{pmatrix} \mathbb{V}_2 & 0 & \mathbb{V}_{57} & 0 \\ 0 & \mathbb{V}_2 & 0 & -\mathbb{V}_{57} \\ \mathbb{V}_{57} & 0 & \mathbb{V}_2 & 0 \\ 0 & -\mathbb{V}_{57} & 0 & \mathbb{V}_2 \end{pmatrix}, \tag{31}$$

where

$$\mathbb{V}_1 = \frac{\kappa C\cosh(2r) + (1+2n_{\text{th}})(\kappa+\gamma+\gamma C)}{2(\kappa+\gamma)(1+C)},$$
$$\mathbb{V}_{13} = \frac{\kappa C\sinh(2r)}{2(\kappa+\gamma)(1+C)}, \tag{32}$$
$$\mathbb{V}_2 = \frac{(\kappa+\gamma+\kappa C)\cosh(2r) + (1+2n_{\text{th}})\gamma C}{2(\kappa+\gamma)(1+C)},$$
$$\mathbb{V}_{57} = \frac{(\kappa+\gamma+\kappa C)\sinh(2r)}{2(\kappa+\gamma)(1+C)}. \tag{33}$$

The opto-mechanical cooperativity C is given by[10]

$$C = \frac{4\mathcal{G}^2}{\gamma\kappa} = \frac{8\omega_a^2}{m\gamma\omega_M\omega_L L^2}\frac{\mathcal{P}}{[(\kappa/2)^2+\omega_M^2]}. \tag{34}$$

The covariance matrices given in Eq. (31) can also be written, for the two-mode symmetric squeezed thermal states, in the following compact matrix form

$$\mathcal{V}_{(j)} = \begin{pmatrix} s & 0 & k & 0 \\ 0 & s & 0 & -k \\ k & 0 & s & 0 \\ 0 & -k & 0 & s \end{pmatrix} \equiv \begin{pmatrix} \mathcal{S} & \mathcal{K} \\ \mathcal{K}^T & \mathcal{S} \end{pmatrix}. \tag{35}$$

In Eq. (35), the index j represents a subsystem m_1m_2 (mirror 1 and mirror 2 modes) or o_1o_2 (optic 1 and optic 2 modes) and the matrix blocks $\mathcal{S} = \operatorname{diag}(s,s)$ and $\mathcal{K} = \operatorname{diag}(k,-k)$ are the covariance matrix 2×2 respectively describing the single mode and the nonclassical correlations between the mechanical and optical modes. For subsystem m_1m_2 ($s = \mathbb{V}_1$ and $k = \mathbb{V}_{13}$) and for subsystem o_1o_2 ($s = \mathbb{V}_2$ and $k = \mathbb{V}_{57}$).

5. Gaussian intrinsic entanglement and purity

In this section, we will study the entanglement of the mechanical ($m_1 - m_2$) and optical ($o_1 - o_2$) modes in the symmetrical state by using the Gaussian intrinsic entanglement (GIE) and the purity. For the two-mode Gaussian states with continuous variables (CV), the Gaussian intrinsic entanglement is defined in Ref. [25]. For the symmetric squeezed thermal states with the covariance matrix given by (Eq. (35)), the Gaussian intrinsic entanglement is[25]

$$E_{\downarrow}^{G} = \begin{cases} \operatorname{Ln}\left[\dfrac{4(s-k)^2+1}{4(s-k)}\right], & \text{iff } s < k+1/2 \text{ and } s < 1.205, \\ 0, & \text{iff } s \geq k+1/2. \end{cases} \tag{36}$$

The condition of entanglement of the two modes is $E_{\downarrow}^{G} > 0$, therefore if $E_{\downarrow}^{G} = 0$, the two modes are separable.

The purity of the two modes is given by[26,27]

$$\mu^{(j)} = \frac{1}{4\sqrt{\det \mathbb{V}_{(j)}}}, \tag{37}$$

where the index j represents a subsystem m_1m_2 (mirror 1 and mirror 2 modes) or o_1o_2 (optic 1 and optic 2 modes). The purity $\mu^{(j)}$ is a witness of the mixedness of the Gaussian state with $0 \leq \mu^{(j)} \leq 1$: the state of the two modes is mixed if $\mu^{(j)} < 1$, and is pure if $\mu^{(j)} = 1$.

The explicit expression of the purity for mechanical and optical modes is written respectively

$$\mu^{m_1m_2} = \frac{(1+C)^2(\kappa+\gamma)^2}{[(1+2n_{\text{th}})(\kappa+\gamma(1+C)) + \kappa C\cosh(2r)]^2 - \kappa^2C^2\sinh^2(2r)}, \tag{38}$$

$$\mu^{o_1o_2} = \frac{(1+C)^2(\kappa+\gamma)^2}{(\kappa+\gamma)(\kappa+\gamma+2\kappa C) + C^2(\kappa^2+\gamma^2(1+2n_{\text{th}})^2) + 2\gamma C(1+2n_{\text{th}})(\kappa+\gamma+\kappa C)\cosh(2r)}. \tag{39}$$

If $r = 0$ and $n_{\rm th} = 0$, equations (38) and (39) lead to the maximum value of purity, *i.e.*, $\mu^{m_1m_2} = 1$ and $\mu^{o_1o_2} = 1$.

We consider recent experimental parameters:[41] The laser frequency $\omega_L/2\pi = 2.82\times10^{14}$ Hz ($\lambda = 1064$ nm). The cavity length and frequency are respectively $L = 25$ mm and $\omega_a/2\pi = 5.26\times10^{14}$ Hz. The movable mirrors oscillate with frequency $\omega_M/2\pi = 947\times10^3$ Hz, the mechanical damping rate $\gamma/2\pi = 140$ Hz and having the mass $m = 145$ ng.

In Fig. 2, we show the evolution of GIE of the mechanical modes (a) and optical modes (b) as a function of the thermal bath photons number $n_{\rm th}$ for various values of the squeezing parameter r with a fixed values of C and γ/κ. When the GIE disappears, the two modes are not entangled. It is clear that, when the parameter r is equal to zero ($r = 0$), the two subsystems remain separable, as shown in Fig. 2. For a fixed value of photons number $n_{\rm th}$, the generation of the entanglement between, on the one hand, the mirror–mirror modes (see Fig. 2(a)) and, on the other hand, between the optic–optic modes (see Fig. 2(b)) improves with the increase of the parameter r ($r > 0$). This shows the dependence between the entanglement and the squeezing parameter r, as in Ref. [12]. In addition, figure 2 shows that for a given r ($r > 0$), the two optical modes (Fig. 2(b) remain entangled over a wider range of $n_{\rm th}$ than the two mechanical modes (Fig. 2(a)). We can also see that movable mirrors and optical modes become separable when the photons number is around $n_{\rm th} \geq 4$ and $n_{\rm th} \geq 6.5$ respectively. Since the number of photons is directly related to the temperature, we can deduce that the optical modes remain entangled over a wider temperature range than the mechanical modes. This effect of temperature is the sign of decoherence.[18] Note also that as the photons number increases, the entanglement decreases quickly which means that the transfer of quantum correlations from two-mode light to the mechanical modes decreases monotonically. This phenomenon can also be explained by the concept of entanglement sudden death (ESD) as in Ref. [19].

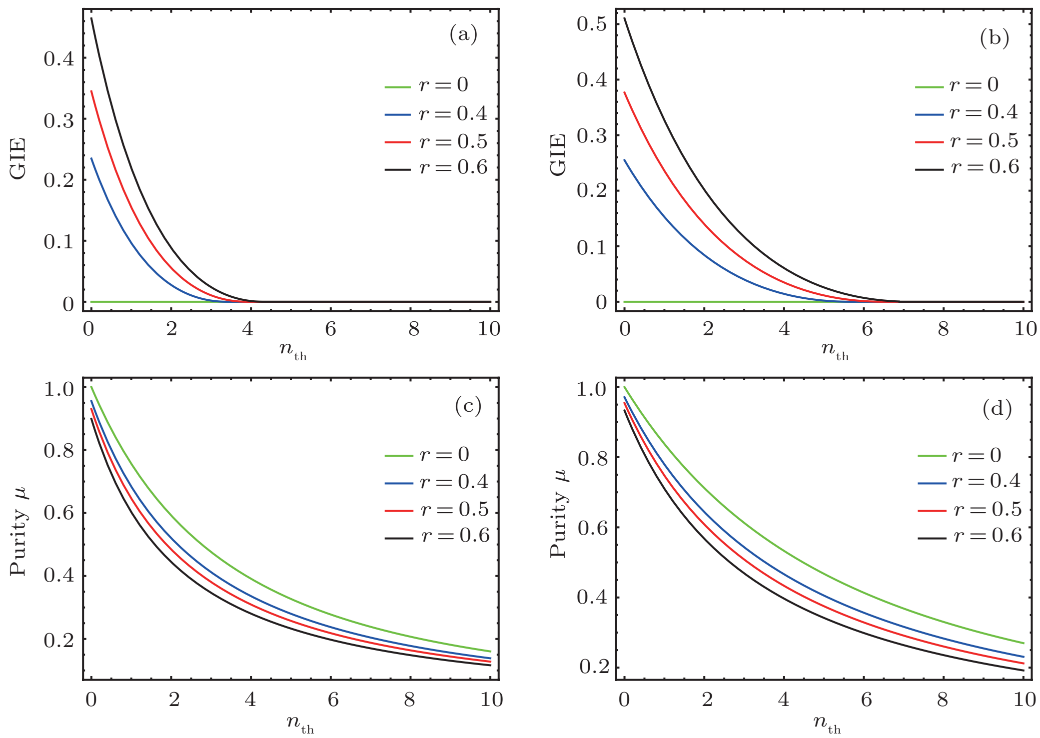

Fig. 2. Plots of GIE [(a) and (b)] and purity μ [(c) and (d)] of the two subsystems *versus* the thermal bath photon numbers $n_{\rm th}$ for different values of the squeezing parameter r: (a)–(c): mirror 1–mirror 2; (b)–(d): optic 1–optic 2. The optomechanical cooperativity is $C = 34$ and $\kappa = 20\gamma$.

In Figs. 2(c) and 2(d), we plot the evolution of the purity respectively of mirror–mirror modes and field–field modes as a function of thermal bath photon numbers $n_{\rm th}$ for different values of r. It is clear that for the two subsystems, the purity reaches its maximum value ($\mu^{m_1m_2} = 1$, $\mu^{o_1o_2} = 1$) when $r = 0$ and $n_{\rm th} = 0$, according to Eqs. (38) and (39); then it decreases when the number of photons $n_{\rm th}$ increases. We notice that the witness of mixedness increases with increasing thermal effect, and also with increasing squeezing parameter r, but the entanglement between the two mechanical modes and the entanglement between the two optical modes increase with increasing r. Indeed, for a fixed value of $r > 0$, when the purity increases also the entanglement increases as illustrate in Figs. 2(a)–2(c) and Figs. 2(b)–2(d). The comparison between Figs. 2(c) and 2(d) shows for $r > 0$ that the purity of optical modes remains superior for a wider range of temperature than mechanical modes, this may explain why optical modes remain entangled for a wider range of $n_{\rm th}$ than mechanical modes as in Figs. 2(a) and 2(b). For example, when $r = 0.5$ and $n_{\rm th} \approx 2$, we have GIE ≈ 0.06 for mechanical modes, and GIE ≈ 0.14 for optical modes. This finding can also be explained by the phenomenon of decoherence.

We remark also the importance of studying the effect of optomechanical cooperativity on the evolution of the entanglement between mechanical and optical modes. Figure 3(a) shows, for a fixed values of r and γ/κ, that there exists a minimum optomechanical cooperativity $C_{\min}$ (*i.e.*, $C > C_{\min}$) for which the mechanical modes (movable mirrors) start entangled if $n_{\rm th} < 5$ (*i.e.*, the entanglement is vanishing if $n_{\rm th} \geq 5$). We observe that the entanglement (GIE) between mechanical modes increases with the increase of C for a fixed value of $n_{\rm th}$, whereas for a given C, the GIE decreases with the increase of $n_{\rm th}$ (see Fig. 3(a). Moreover, the value of $C_{\min}$, which corresponds to the birth of the entanglement of the mechanical modes, increases with the increase of $n_{\rm th}$ (see Fig. 3(a)); this is explained by the effect of the decoherence on the entanglement of the two mobile mirrors.

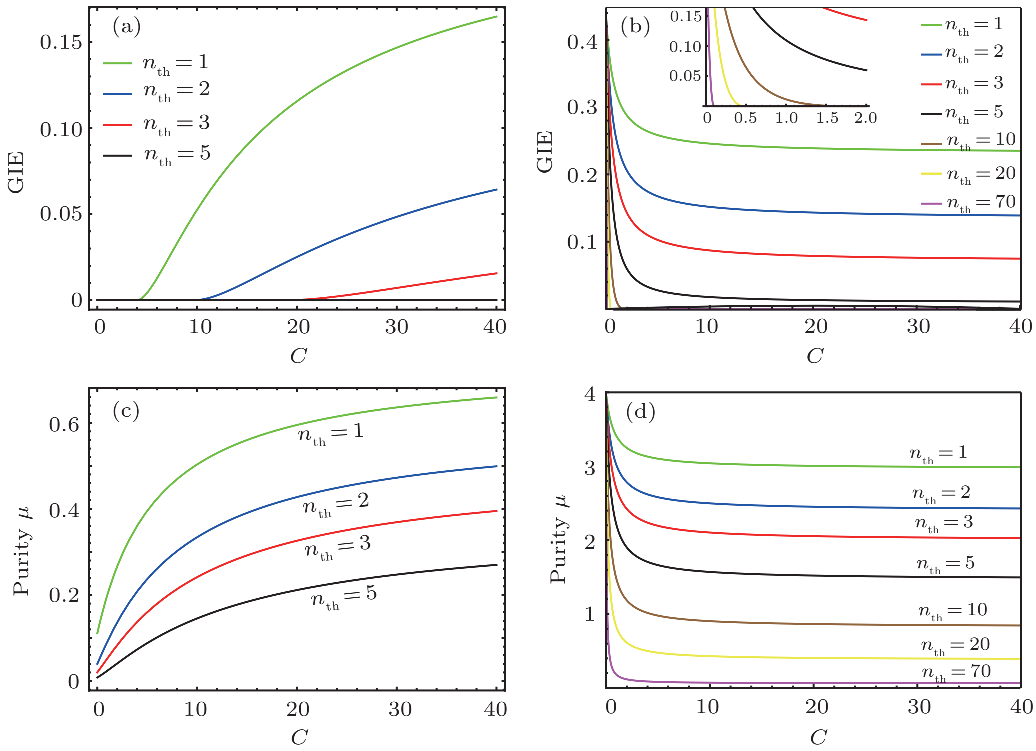

Fig. 3. Plots of GIE [(a) and (b)] and purity μ [(c) and (d)] of the two subsystems *versus* the optomechanical cooperativity C for various values of the thermal bath photon numbers $n_{\rm th}$. (a)–(c): Mirror 1–mirror 2; (b)–(d): optic 1–optic 2 with $r = 0.5$ and $\kappa = 20\gamma$.

Figure 3(b) shows that the optical modes are entangled even if $n_{\rm th} \geq 5$, but mechanical modes are separable (see Fig. 3(a)). Moreover, when $n_{\rm th}$ increases, we note that there exists a maximum value of the optomechanical cooperativity ($C < C_{\max}$) for which the optical modes are entangled. It is clear that the increase in the photons number $n_{\rm th}$ causes the decrease of $C_{\max}$, for a given $n_{\rm th}$ the GIE decreases with increasing optomechanical cooperativity, whereas when C is fixed, the GIE increases with decrease of $n_{\rm th}$.

Figures 3(c) and 3(d) illustrate the evolution of the purity of the mirror 1–mirror 2 and optic 1–optic 2 subsystems respectively with respect to the optomechanical cooperativity for different values of $n_{\rm th}$. For the two subsystems, the figures show that the purity decreases with the increase of $n_{\rm th}$, as it is clear from Eqs. (38) and (39), this due to the decoherence phenomenon. Remarkably, for mobile mirrors, purity increases very rapidly with C increases. In the case of optical modes, we observe a rapid decrease in purity for low values of C followed by a small variation and then it seems to stabilize for the large values of C (see Fig. 3(d)). Finally, following Fig. 3, we can conclude that the transfer of quantum correlations from the two-modes squeezed light to the mechanical modes has the effect of improving entanglement (when $C > C_{\min}$) and purity; but for both optical modes, the effect is reversed.

6. Gaussian discord with the Hellinger distance

In this section, we will study the progress of Gaussian geometric discord in terms of Hellinger distance (GGD-Hd), in order to characterize the quantum correlations in bipartite Gaussian states,[28] using RWA. The two subsystems (mirror–mirror and optic–optic) are described by the covariance matrices, *e.g.*, Eqs. (31) and (35), the explicit expression of GGD-Hd for the two-modes symmetric squeezed thermal states is given by[28]

$$D_{\mathrm{H}}^{(j)} = 1 - \frac{4(\det(\mathbb{V}_{(j)}))^{1/4}}{2s + 2(\det(\mathbb{V}_{(j)}))^{1/4}(\sqrt{N_1} - \sqrt{N_2})}, \tag{40}$$

where the index j represents a subsystem m_1m_2 (mirror 1 and mirror 2 modes) or o_1o_2 (optic 1 and optic 2 modes) with $N_1 = (\lambda_1 + 1/2)^2$, $N_2 = (\lambda_2 - 1/2)^2$, and $\lambda_1 = \lambda_2 = \sqrt{s^2 - k^2}$ being the symplectic eigenvalues of the covariance matrices Eqs. (31) and (35), with $s = \mathbb{V}_1$ and $k = \mathbb{V}_{13}$ for mirror–mirror subsystem, and $s = \mathbb{V}_2$ and $k = \mathbb{V}_{57}$ for optic–optic subsystem.

Figures 4(a) and 4(b) represent respectively the evolution of GGD-Hd of the two mirror–mirror and optical–optical subsystems as a function of the thermal bath photons numbers n_{th} for different values of the squeezing parameter r with fixed values of C and γ/κ parameters. Indeed, when $r = 0$ the quantum correlations are not transferred between the two modes; this shows the strong relationship between squeezed light and quantum correlations. These figures show that GGD-Hd degrades with the increase of n_{th}, but improves by increasing the parameter r. The comparison between Figs. 2(a) and Figs. 4(a) and 4(b) allows us to notice that when the two subsystems (mechanical or optical) are no longer entangled, GGD-Hd does not disappear. Therefore, GGD-Hd can quantify quantum correlations beyond entanglement. For example, when $n_{\mathrm{th}} = 6$ and $r = 0.5$, we have GIE=0 while GGD-Hd ≈ 0.08 for the two mechanical modes.

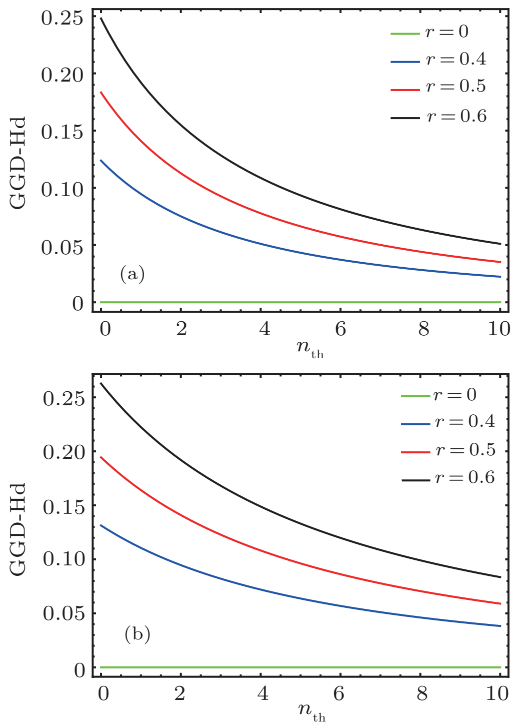

Fig. 4. Plots of the Gaussian Hellinger discord (GGD-Hd) of the two subsystems *versus* the thermal bath photon numbers n_{th} for different values of the squeezing parameter r: (a) mirror 1–mirror 2, (b) optic 1–optic 2. The optomechanical cooperativity is $C = 34$ and $\kappa = 20\gamma$.

Figures 5(a) and 5(b) show respectively the effect of optomechanical cooperativity C on the GGD-Hd of the mirror–mirror and optical–optical subsystems for various values of the thermal bath photons numbers n_{th} with fixed values of r and γ/κ. It is clear that, for the mechanical modes, the GGD-Hd decreases with the increase of n_{th}, whereas it increases with the increase of C (Fig. 5(a)). For the optical modes, on the one hand, the GGD-Hd decreases with the increase of n_{th}; this shows the effect of the thermal bath temperature which is proportional to the number of photons. On the other hand, the GGD-Hd exhibits a very rapid degradation with the increase of C, then seems to keep a stable value after a certain value of C which is less than 4 (Fig. 5(b). This behavior can be explained by the freezing phenomenon that has also been discussed in Ref. [42]. The comparison between Fig. 5 and Fig. 3 shows us that, when the mechanical and optical modes are separable, the GGD-Hd remains non-zero. Therefore, we can conclude that GGD-Hd is more robust than Gaussian intrinsic entanglement (GIE) under the thermal effect. In other words, GGD-Hd measures the total quantum correlations even if the two modes are not entangled under the thermal effect.

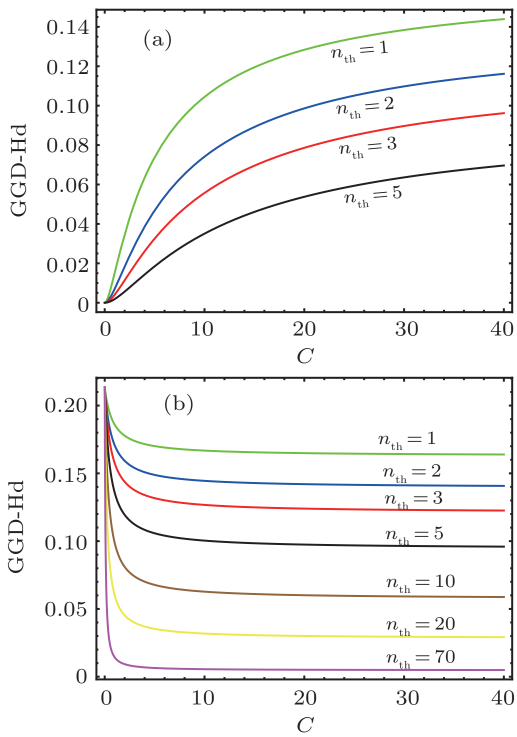

Fig. 5. Plots of the Gaussian–Hellinger discord (GGD-Hd) of the two subsystems *versus* the optomechanical cooperativity C for various values of the thermal bath photon numbers n_{th}: (a) mirror 1–mirror 2, (b) optic 1–optic 2 with $r = 0.5$ and $\kappa = 20\gamma$.

7. Conclusion

In summary, we have studied and compared entanglement, purity and Gaussian geometric discord in terms of Hellinger distance in an optomechanical system in the Gaussian state of continuous variables. The system consists of two spatially separated Fabry–Pérot cavities. Each cavity has a fixed mirror and a movable mirror, and is powered by two-mode squeezed light source and a coherent laser source. After giving the Hamiltonian expression and the non-linearized quantum Langevin equations, we derived the linearized quantum Langevin equations describing the dynamics of the system by considering the linearization scheme. Using the rotating wave approximation, we derived the explicit expression of the covariance matrix Eq. (30) of the Gaussian stationary state for the mechanical modes and the optical modes. We have used Gaussian intrinsic entanglement of two-mode continuous variables Gaussian states to quantify the amount of entanglement between mechanical and optical modes at strong coupling under thermal effect, which allowed us to highlight the phenomenon of sudden death entanglement under thermal effect. We have also shown the influence of various factors, such as temperature T, squeezing parameter r and optomechanical cooperativity C on entanglement generation. The analysis of purity as a witness of the mixing between the mechanical and optical modes, has shown that the purity is degraded under the thermal effect. The general nonclassical correlations were also quantified using Gaussian geometric discord in terms of Hellinger distance (GGD-Hd). We have found that GGD-Hd is more robust than entanglement for mechanical and optical modes under thermal effect. Indeed, this thermal effect lead to decoherence phenomenon, which remains a major challenge for information and quantum processing.

References

[1] Einstein A, Podolsky B and Rosen N 1935 *Phys. Rev.* **47** 777
[2] Schrödinger E 1935 *Proc. Cambridge Philos. Soc.* **31** 553
[3] Bell J S 1964 *Physics* **1** 195
[4] Bennett C H, Brassard G, Crepeau C, Jozsa R, Peres A and Wootters W K 1993 *Phys. Rev. Lett.* **70** 1895
[5] Bennett C H and Wiesner S J 1992 *Phys. Rev. Lett.* **69** 2881
[6] Scarani V, Lblisdir S, Gisin N and Acin A 2005 *Rev. Mod. Phys.* **77** 1225
[7] Ekert A K 1991 *Phys. Rev. Lett.* **67** 661
[8] Shi H and Bhattacharya M 2016 *J. Phys. B : At. Mol. Opt. Phys.* **49** 153001.
[9] Bowen W P and Milburn G J 2016 *Quantum* Optomechanics
[10] Aspelmeyer M, Kippenberg T J and Marquardt F 2014 *Rev. Mod. Phys.* **86** 1391
[11] Agarwal G S and Huang S 2010 *Phys. Rev. A* **81** 041803
[12] Sete E A, Eleuch H and Ooi C H R 2014 *J. Opt. Soc. Am. B* **31** 2821
[13] Suciu S and Isar A 2015 *AIP Conference Proceedings* **1694** 020013
[14] Amazioug M, Nassik M and Habiballah N 2018 *Eur. Phys. J. D* **72** 171
[15] Amazioug M, Nassik M and Habiballah N 2018 *Optik-Int. J. Light Elect. Opt.* **158** 1186
[16] Amazioug M, Nassik M and Habiballah N 2018 *Int. J. Quantum Inform.* **16** 1850043
[17] Amazioug M, Nassik M and Habiballah N 2019 *Chin. J. Phys.* **58** 1
[18] Zurek W H 2003 *Rev. Mod. Phys.* **75** 715
[19] AlQasimi A and James D F V 2008 *Phys. Rev. A* **77** 12117
[20] Yu T and Eberly J H 2004 *Phys. Rev. Lett.* **93** 140404
[21] Yu T and Eberly J H 2006 *Opt. Commun.* **264** 393
[22] Yu T and Eberly J H 2006 *Phys. Rev. Lett.* **97** 140403
[23] Yu T and Eberly J H 2009 *Science* **323** 598
[24] Almeida M P, de Melo F, Hor-Meyll M, Salles A, Walborn S P, Souto Ribeiro P H and Davidovich L 2007 *Science* **316** 579
[25] Mista L Jr and Tatham R 2016 *Phys. Rev. Lett.* **117** 240505
[26] Paris M G A, Illuminati F, Serafini A and De Siena S 2003 *Phys. Rev. A* **68** 012314
[27] Adesso G, Serafini A and Illuminati F 2004 *Phys. Rev. Lett.* **92** 087901
[28] Marian P and Marian T A 2015 *J. Phys. A : Math. Theor.* **48** 115301
[29] Tian L and Wang H 2010 *Phys. Rev. A* **82** 053806
[30] Wang Y D and Clerk A A 2012 *Phys. Rev. Lett.* **108** 153603
[31] Pinard M, Dantan A, Vitali D, Arcizet O, Briant T and Heidmann A 2005 *Europhys. Lett.* **72** 747
[32] Giovannetti V and Vitali D 2001 *Phys. Rev. A* **63** 023812
[33] Gardiner C W and Zoller P 2000 *Quantum Noise* **p.** 71
[34] Gardiner C W 1986 *Phys. Rev. Lett.* **56** 1917
[35] Sete E A, Eleuch H and Das S 2011 *Phys. Rev. A* **84** 053817
[36] Wang Y D, Chesi S and Clerk A A 2015 *Phys. Rev. A* **91** 013807
[37] Mari A and Eisert J 2009 *Phys. Rev. Lett.* **103** 213603
[38] DeJesus E X and Kaufman C 1987 *Phys. Rev. A* **35** 5288
[39] Vitali D, Gigan S, Ferreira A, B?hm H R, Tombesi P, Guerreiro A, Vedral V, Zeilinger A and Aspelmeyer M 2007 *Phys. Rev. Lett.* **98** 030405
[40] Parks P C and Hahn V 1993 *Stability* Theory
[41] Gröblacher S, Hammerer K, Vanner M R and Aspelmeyer M 2009 *Nature* **460** 724
[42] El Qars J, Daoud M and Ahl Laamara R 2018 *J. Mod. Opt.* **65** 1584